3rd Specialty Conference on Material Engineering & Applied Mechanics
3e Conférence spécialisée sur le génie des matériaux et mécanique appliquée

Montréal, Québec
May 29 to June 1, 2013 / *29 mai au 1 juin 2013*

Finite Element Modelling of Welding Procedures in High Strength W-Shapes

Violetta Nikolaidou, Colin A. Rogers, Dimitrios G. Lignos
Department of Civil Engineering and Applied Mechanics, McGill University, Montreal

Abstract: The use of high strength stocky steel columns has become more frequent in modern steel construction due to seismic and blast design requirements. When these columns are used as part of prequalified beam-to-column connections having thick doubler plates, in order to provide sufficient panel zone shear strength, there may be a large potential for crack initiation related to the welding. This paper discusses the development of a detailed finite element model that simulates flux core arc welding with a gas shield (FCAW-G) of thick doubler plates on a high strength A 913 Gr. 65 W-Shape with complete joint penetration flare bevel groove welds. Finite element simulation results are presented for the heat transfer and stress analysis that replicates the welding sequence that is currently used in practice.

1 Introduction

Prequalified beam-to-column connections are widely used to enhance building resistance to earthquake or blast loading. In order to increase the shear strength of the panel zones, thick doubler plates are typically welded to the web of the column. In addition, the ever-growing demand for taller buildings and longer spans has led to the increased use of high strength steel shapes as part of the construction process. Therefore, the need to investigate the behaviour of welded connections to these sections proves crucial in avoiding connection failure and improving currently used welding techniques in practice. Figure 1 shows a thick doubler plate welded at the beam-to-column connection location of a high strength (65 ksi / 450 MPa) wide flange W-Shape column 8131mm long.

Figure 1: Prequalified connection in high strength (65 ksi / 450 MPa) W-Shape

During the welding process of the doubler plate to the web of a column, melting and cooling of the weld and base metal take place by applying locally a considerable concentrated amount of heat through the use of a transient heat source. The base metal being in the vicinity of the weld is mostly affected because its properties change due to the increase of temperature (increased level of hardness). This region is referred to as the heat-affected zone. The performance of the resulting weld depends on many

parameters such as the electrode used and the experience of the operator, with the most significant parameters being the welding procedure (including pre- and post-heating) and the welding sequence. Discontinuities and cracking may occur both in the weld metal and the heat-affected zone of the base metal. Two main reasons exist for the occurrence of discontinuities after the completion of the welding process; poor weld design and residual stresses. The former refers to discontinuities such as undercut, lack of fusion and incomplete penetration, while the latter is introduced through solidification, cooling and weld shrinkage (Blodgett et al. 1999). The failures described here occurred during or soon after fabrication and were not due to in-service loading.

Most cracks occur due to shrinkage of the weld metal while cooling; a non-uniform process that takes place inside the weld. Tensile residual stresses are introduced both inside the weld bead and between the weld bead and the heat-affected zone. The larger the weld the larger the shrinkage and the stresses introduced to the weld location and the areas adjacent to it. Therefore this issue is magnified in multi-pass welding. Tensile residual stresses can influence greatly the global behaviour of the welded structure as they soften the material, making it susceptible to early yielding and even fracture failure. To this end, many studies of the last two decades were carried out to better understand and predict the residual stress distribution (Ma et al. 1995, Teng et al. 2001, Siddique et al. 2005). Because of the complexity of the welding process due to the various parameters that it involves, accurate prediction of residual stresses raised many difficulties, which led to the use of advanced finite element modelling of the welding procedures. Recent studies involve finite element modelling in T-joint fillet welds, butt-welded plates and high strength steel plate to plate joints (Vakili-Tahami et al. 2008, Chang et al. 2009, Jin et al. 2011). However, there appears to be a lack of information concerning finite element modelling of multi-pass welding procedures on high strength sections involving real life structural components and practical problems encountered in practice related to residual stresses due to the welding processes.

This paper discusses the development of a two-dimensional (2D) finite element (FE) model, which simulates the flux core arc welding process with a CO_2 gas shield (FCAW-G) of thick doubler plates on a high strength A 913 Gr. 65 W-Shape with complete joint penetration flare bevel groove welds. Based on information from the steel industry, cracks have occurred in the column flanges near the flange to web junction of high strength W-Shape columns right after all welding procedures were completed. For this reason the main focus of the paper is on the flange regions of these pre-qualified connections. The cracks were observed in the column flange after misplaced shear tabs at these locations were removed. Gouging of the flange was completed in order to trace and remove the crack; however, an attempt to repair the two columns was unsuccessful. Figure 2a illustrates the gouged flange of the column and Figure 2b shows the same flange after the attempted repair procedure. The intent of developing the FE model was to be able to explain how the welding process influenced the development of the cracks and to make recommendations as to how best to modify the procedure such that this type of fabrication related damage could be avoided. This paper contains a presentation of the initial Abaqus FE (Abaqus FEA/CAE 2011) modelling of the welding procedure.

(a) Gouged Flange (b) Repaired Flange

Figure 2: Efforts to repair columns at crack locations

2 FE Modelling Procedure

2.1 Geometry and Meshing

Two 25mm thick, 286x1332mm doubler plates were welded to the web of a W360x237 (W14x159) column section at the beam-to-column connection location. The welding process on each side of the web consisted of two 13-pass complete joint penetration (CJP) flare bevel groove welds with weld angle 30^{o} performed at the k-areas and two 6-pass plug welds at the middle (Figure 3). The steel column was supported by two rigid bodies at the tip of its flanges to represent the actual supports of the column during welding in the fabrication shop. The numerical model consisted of four parts; (1) the W-Shape with the welds; (2) the upper doubler plate; (3) the lower doubler plate; and (4) the flange supports (ref.p.1 and ref.p.2 refer to reference points added in the model as part of the rigid body constraints).

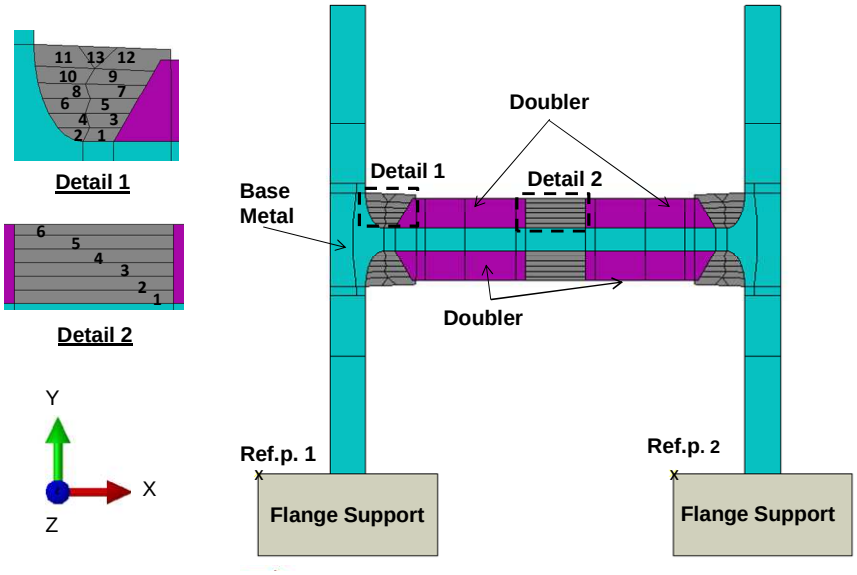

Figure 3: 2D model geometry of the prequalified connection

It should be mentioned that the doubler plates were also welded along the other two edges in the other direction with 1-pass fillet welds using the same welding process. However, the model simulated a cross section through the fabricated column therefore these welds were not part of the model and, thus, they are not shown in Figure 3. The same applies for the second plug weld. Nonetheless, the corresponding construction time for these welds was taken into account, as explained in Section 2.2.1.

The W-shape and doubler plates were fabricated from A 913 Gr. 65 and A 572 Gr. 50 steel, respectively. In order to simulate the nonlinear behaviour of the steel materials, a bilinear model was employed with 3% strain hardening. For the A 913 Gr. 65 steel, the yield stress at 15^{o}C was assumed to be 516MPa based on mill tests provided from the industry. Similarly, for the A 572 Gr. 50 steel, the yield stress was assumed to be 380MPa (expected yield stress). A nominal value of 400MPa was chosen as the yield stress of the weld metal for an E70 electrode at room temperature. The reduction of the yield stress and Young's modulus as a function of the temperature increase was taken into account based on Eurocode 3, Design of steel structures Part 1-2 (Eurocode-3, CEN 2003) (Figure 4). Note that after 1000^{o}C the material has practically zero yield stress and axial rigidity.

The FE meshing arrangement of the 2D cross-section is shown in Figure 5. Quadrilateral and quadratic elements were selected, with a minimum element size of 2mm. Heat transfer and plane strain 8-node quadratic quadrilateral elements were implemented for the heat transfer and stress analysis, respectively.

Heat transfer elements have only temperature as a degree of freedom; the nodal temperature values are saved as output and inserted as input in the stress analysis. Plane strain elements are suitable for a 2D stress analysis where residual stresses (out-of-plane stresses) and in-plane strain distributions are of interest.

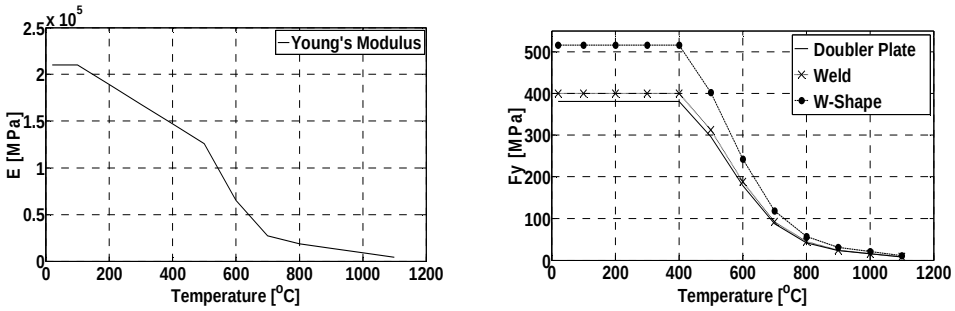

(a) Young's modulus E (b) Yield stress F_y

Figure 4: Assumed reduction of material properties due to temperature increase based on Eurocode 3

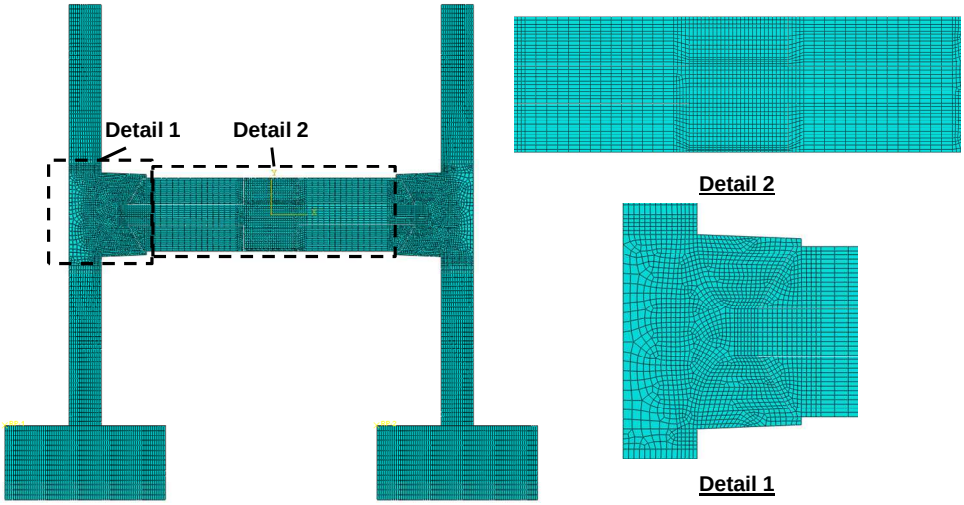

Figure 5: FE mesh of the W-Shape, the doubler plates and the welds

The width of the heat-affected zone was assumed to be 8mm near the weld and 16mm under the weld. In those regions the meshing was denser than in the area of the model between the CJP and plug welds and the CJP and the tips of the flanges, as shown in Figure 5. It should be noted that the flanges had an equal mesh density to the HAZ, but this was due to the contact elements inserted between the flange tips and their rigid supports.This assumption, regarding the width of the HAZ, was based on recent studies, where the effect of the weld bead on the material properties of the base metal for different welding processes was examined using micrography (Gunaraj & Murugan 2002, Aloraier et al. 2006, Aloraiera et al. 2010, Lee et al. 2007, Mark et al. 2012). In these studies the range of the heat-affected zone was found to be from 4 to 6mm under the weld and 2mm near the weld.

The welding sequence typically used in practice involves completion of all welding passes on the one side of the web of the W-Shape, both plug and flare bevel welds. The column is then flipped and the welds on the other side of the web are performed. Based on this process, the finite element modelling discussed as part of this paper consisted of a heat transfer and stress analysis performed for one side of the web for the welding of one doubler plate. The same analyses with the exact same steps was then repeated for the other side of the web and the welding of the second doubler plate with an additional step at the

beginning where the results from the first two analyses were inserted as initial conditions for the next two analyses. A detailed description of the heat transfer and stress analysis modelling procedure is presented referring to the welding procedures for one doubler plate on the one side of the web of the steel column.

2.2 Heat Transfer Analysis

A heat transfer analysis was conducted as part of the proposed finite element model. Coupling of mechanical and thermal effects was neglected, meaning that the temperature distribution of the steel material adjacent to the weld was calculated without considering stresses and deformations in the model. This is attributed to the fact that in the welding process simulation the stress field is dependent on the temperature distribution but the inverse does not apply. This type of analysis includes conduction, boundary convection and boundary radiation allowing the transfer and exchange of temperature between surfaces in contact and with the environment. Latent heat effects (between phase changes) were not included, given the small volume (welding pass and small area around it) that changes phase during the welding process. The temperature boundaries chosen, based on feedback from the industry, were 15^{o}C low temperature (ambient temperature) and 1500^{o}C high temperature (temperature during welding). The specific heat coefficient and thermal conductivity (fully isotropic) varied with temperature as shown in Figure 6. The phase transformation of metal (at 723^{o}C) was taken into account in these graphs. Additional information regarding material properties inserted in the model, such as thermal expansion, can be found in Eurocode 3, Design of steel structures Part 1-2.

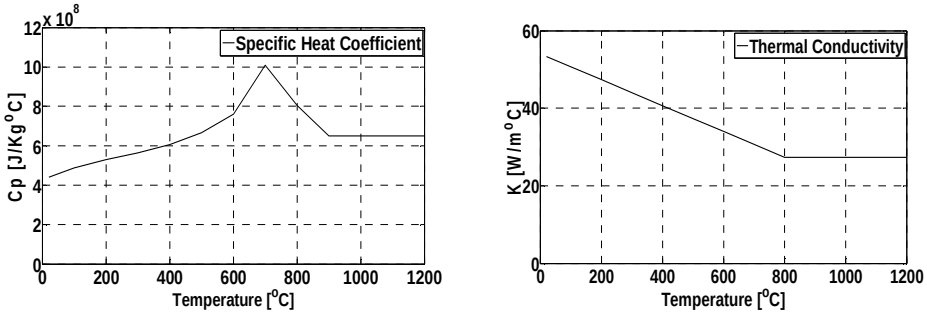

(a) Specific Heat Coefficient (b) Thermal Conductivity

Figure 6: Specific heat and thermal conductivity as a function of temperature (Eurocode-3, CEN 2003).

The boundary conditions of the finite element model included a prescribed temperature, surface heat flux and volumetric heat flux with surface convection given by Equation 1 and radiation by Equation 2.

[1] $q = h(\theta-\theta^{o})$, where $h = h(x,t)$ is the film coefficient and $\theta^{o} = \theta^{o}(x,t)$ is the sink temperature (15^{o}C).

[2] $q=A((\theta-\theta^{z})^4 – (\theta^{o} – \theta^{z})^4)$, where A is the radiation constant (emissivity (0.625, constant from Eurocode) times the Stefan-Boltzman constant (5.67E-011)) and θ^{z} is the value of absolute zero (-273 ^{o}C).

2.2.1 Welding Sequence and Modelling Parameters

As mentioned, the welding sequence performed for the connection of one doubler plate to the web of the W-shape consisted of two plug welds in the middle of the web and two edge complete joint penetration flare bevel groove welds (see Figure 3). In the 2D model, as already mentioned, only one plug weld in the middle is shown but the construction time for both plug welds was taken into account. Based on industry feedback, first a sealing pass was performed around the doubler plate (pass 1 of weld bead at each edge shown in Figure 3). The welds in the other dimension of the doubler plate are not shown in the 2D model, as explained in Section 2.1, but the time of their construction was also taken into account. At this point it should be noted that the construction time, for the welds that are not shown in Figure 3 and were not part of the model, was considered. The reason was that an accurate cooling time for the passes that were simulated must be inserted in the model, given that during cooling time tensile stresses are applied to the

adjacent parts of the welding pass that is under shrinkage. The construction time of the welding passes that were not included in the model constitutes an additional cooling time for the welding passes in the model that were already conducted. Following the first sealing pass, the 6 passes of the plug welds were completed and, subsequently, the rest of the passes of the edge welds. Specifically, after the second pass of the left edge weld was completed a second pass of the right weld followed, then the third pass of the left weld, the third pass of the right weld and so on. This process was simulated in Abaqus with a total of 99 steps. In the initial step, predefined fields were inserted indicating 15^{o}C as the base metal initial temperature (ambient temperature) and 1500^{o}C as the weld metal initial temperature, referring essentially to the molten metal deposited at the base metal surface during each pass. In the next step all weld passes and the doubler plate on the other side of the web (the side where no welding was taking place) were removed instantaneously using a "Model Change" interaction provided in Abaqus in order to be added again later on according to the welding sequence. Subsequently, preheat was applied to the surfaces that were going to be welded through a temperature boundary condition added in the preheat step. The preheat temperature chosen was 66^{o}C, which was applied for 900sec assuming ramp linear behaviour over a step. These values were chosen based on feedback from professional in practice welders. At every step if a surface were not heated, a film condition and surface radiation interactions were applied ensuring the interaction of each surface with the surroundings. After preheat, the first sealing pass was performed. Every welding pass was simulated using three analysis steps. The first step involved the heating of the surfaces where the molten metal was to be deposited. This was achieved by gradually applying a temperature boundary condition of 1500^{o}C to the relative surfaces over the time of the step. The second step involved the reactivation of the weld pass in question in its solid form and the third step replicated the time between passes when weld and base metal were allowed to cool before the next welding pass. The cooling time also included removing the flux from the pass just conducted. All time steps were based on the actual time needed for welders to complete this type of weld. The characteristic time for the completion of one pass of an edge weld was 300sec, whereas the cooling time was set at 900sec, while for the plug welds 45sec and 225sec, respectively, were used for modeling. During this time the electrode travel speed, the doubler plate dimensions and the time needed to move the equipment were all taken into account. The maximum number of increments was set to 100 or 1000 with maximum increment size equal to the time period and initial and minimum increment size defined manually depending on the sizes required for the analysis to be completed in a successful manner.

2.2.2 Element Birth and Death technique

The ability to remove and add parts of the model in Abaqus is referred to as the element "Birth and Death" technique (Brickstad et al. 1998). Essentially parts of the model are not removed but deactivated (death) using the "Model Change" interaction and they can be reactivated (birth) in a following analysis step. In order for this to be achieved at the beginning of the analysis the model must be complete with all its parts active. For the heat transfer elements, the deactivation of a part sets the thermal conductivity of the corresponding elements to zero, while at the reactivation of the part the thermal conductivity is ramped up from zero over the step. This technique allows the simulation of a welding process where passes are conducted or activated, in modelling terms, one after the other. The use of this technique differed in terms of how it was applied for the heat transfer and the stress analyses. In the heat transfer analysis all welding passes were deactivated at the beginning and reactivated at the appropriate step according to the welding sequence followed. In contrast, in the stress analysis all passes were not removed simultaneously at one analysis step. Each pass remained activated in the model throughout the welding process and was only instantaneously deactivated and activated in between its welding and its cooling step.

2.3 Stress Analysis

After the heat transfer analysis had been completed, the stress analysis corresponding to the same parts welded in the heat transfer analysis was performed. A nonlinear static analysis was conducted that considered geometric nonlinearities. The plasticity model used was not strain-rate dependent, meaning that the rate with which the material was strained did not influence the response of the model under investigation.

2.3.1 Modelling Parameters

The same model used in the heat transfer analysis was then used in the stress analysis by means of changing the element type from heat transfer to plane strain. It was of great importance for the element mesh to remain exactly the same for both analyses because the elements carrying the nodal temperature values needed to remain in the same position in the model. Moreover, constraints and boundary conditions were applied to the numerical model of the steel column with the doubler plates, because adequate stiffness and numerical stability of the model is an indispensable factor for the convergence of a stress analysis. For this reason, a tie constraint was applied to all contact surfaces of independent parts of the assembly. In addition, since in the fabrication shop welding is typically performed while a column is positioned on top of steel supports, placed at certain intervals, a rigid body constraint was used in the model. The rigid body constraints were applied at the rigid body parts (see Figure 3); fixed boundary conditions were applied at their reference points. Between the flange tips and the rigid bodies, tangential behaviour was chosen with a friction formulation penalty and a friction coefficient starting from 0.2, while for the normal behaviour a hard contact and the penalty method were chosen for the linear contact stiffness behaviour. The meshing for the surface of the flange tip was chosen to be denser than the body of the flange in general (as mentioned in Section 2.1) but not entirely different from the surface of the rigid body, given that the latter is the master surface and penetration errors needed to be avoided. Clearance was 1mm, given the dimensions of the W-shape in question. To facilitate the activation of the contact an extra step was inserted in the analysis in which only the self-weight of the structure was linearly applied over the time of the step to the initially existing parts of the model. The contact interaction applied between the web of the W-shape (master surface) and the doubler plates incorporated the same contact characteristics and allowed for the doubler plate to follow the deformation of the web. It also took into account the pressure exerted between the two surfaces during the welding process. In the stress analysis the previously obtained temperature distributions were inserted as loads invoking the appearance of stresses. In particular, each welding pass was simulated with a total of four analysis steps describing the pass construction, deactivation and reactivation and the cooling time before the beginning of the next pass. In the first and last step the temperature distributions corresponding to the construction of the pass and cooling time were inserted as predefined fields, respectively. The time periods of these steps were the same as those used in the corresponding steps of the heat transfer analysis.

2.4 Summary of Preliminary Results

2.4.1 Heat Transfer Analysis Results

The heat transfer analysis provided values of the temperatures expected at each step of the welding process at each location of the model. These values were inserted in the stress analysis as loads so that the residual stresses and deformations of the structure due to the welding process could be obtained. Figure 7a shows the numerical model of the steel column with the doubler plates at the initial step of the analysis when the welds and the lower doubler plate were deactivated.

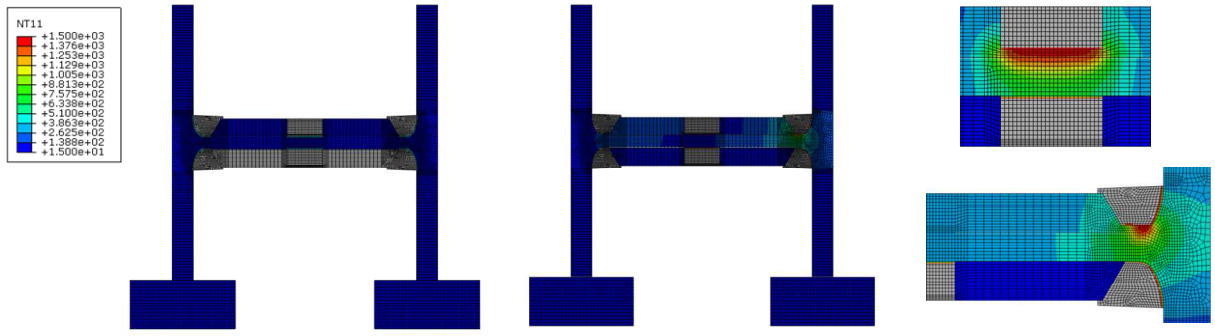

(a) Heat Flux at initial step (b) CJP Pass1 (c) Welding Passes

Figure 7: Snapshots of the activation of welding passes from heat transfer analysis (Temperature in ^{o}C)

During the welding simulation, each pass on the upper side of the web was activated and the temperature was distributed as expected without influencing the lower deactivated parts or the upper welding passes that were still deactivated. This can be seen in Figures 7b and 7c in which snapshots of the activation of welding passes at the plug welds and CJP are shown. The welding pass being conducted is indicated with red. The parts adjacent to the weld that mostly experienced the highest temperatures due to welding are highlighted with green and yellow. Figure 8 shows the temperature distribution immediately after the completion of pass 1 of the left CJP weld and of the first pass at the plug weld. The distance *x* in Figure 8a is measured from the edge of pass 1 of the CJP weld to the edge of the first pass at the plug welds while in Figure 8b from the edge of the first pass at the plug weld to the edge of the pass 1 of the CJP weld (the passes are not included in the distance, only the length of the doubler plate between them).

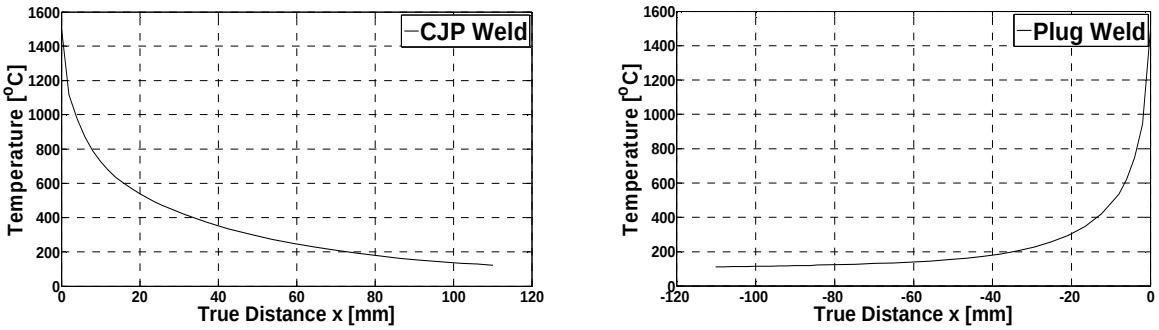

(a) CJP weld (b) Plug weld

Figure 8: Temperature distribution in two different analysis phases

From Figure 8, at least 16mm of base metal adjacent to the weld was subjected to high temperature (nearly 600°C); an indication that the assumption for the width of the HAZ was reasonable. Moreover, the model demonstrated that each welding pass introduced high temperatures in the structure and thus suggested the appearance of considerable stresses upon cooling.

2.4.2 Stress Analysis Results

The results of this preliminary finite element model are presented for the present stage of the stress analysis. Figures 9 and 10 illustrate the stress results on the cross-section, corresponding to the Ux displacements and von Mises stresses, respectively, after the completion of the first welding pass.

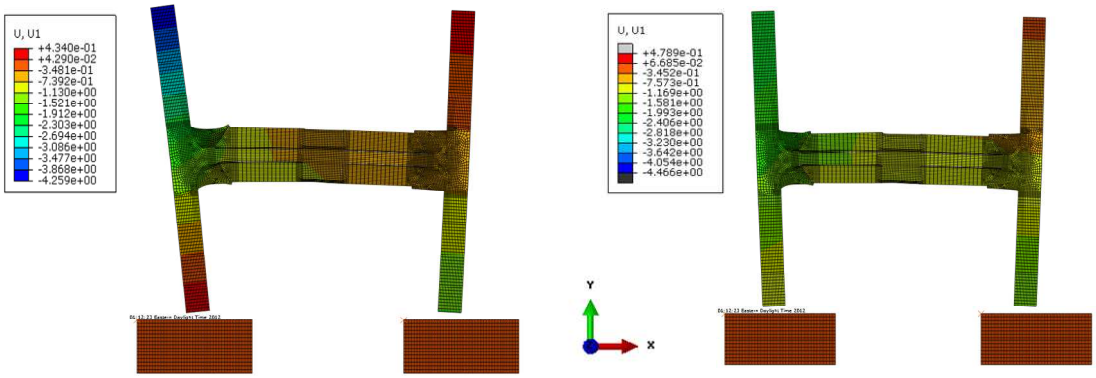

(a) Welding of Pass 1 (b) Resumed Position after Cooling

Figure 9: Stress Analysis results for Ux displacements (mm)

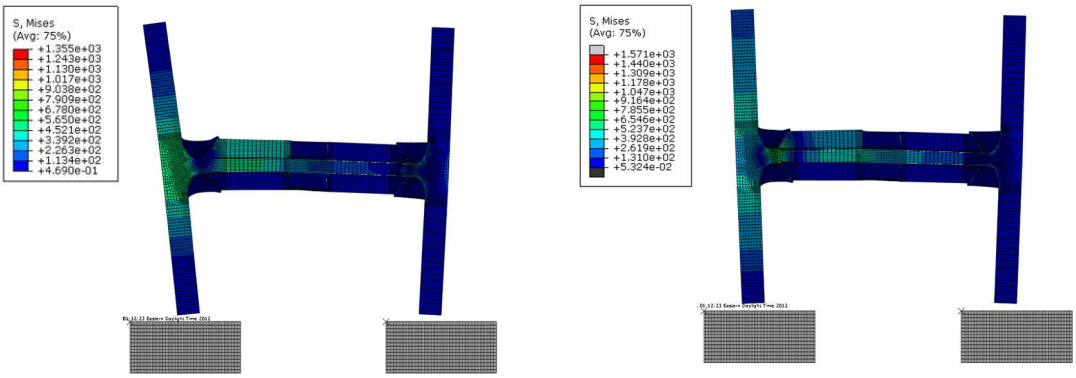

(a) Welding after Pass 1 (b) Resumed Position after Cooling

Figure 10: Stress Analysis results for von Mises stresses (MPa)

Both figures demonstrate how the column flange is expected to deform during the welding of the first pass (Figures 9a, 10a) and how it resumes its position during the cooling time (Figures 9b, 10b). The locally heated location expands and then shrinks back to its previous state when it is allowed to cool.

The next step in this continuing research project is the completion of the stress analysis for all the welding passes such that residual stresses and stresses in the y direction can be obtained in order to examine the possibility of cracks formulating in the flanges due to this welding sequence. This work will be completed in conjunction with a detailed materials testing phase in which coupon and CVN specimens will be obtained from the columns that were found to have cracked after fabrication. Improved materials models will be developed for use in the FE models such that a better evaluation as to the cause of the weld induced cracking can be completed.

3 Summary and Observations

In this study a preliminary FE modelling approach of welding procedures performed on high strength W-Shape columns was presented. Complete joint penetration and plug welds were conducted on the web of a column section, connecting it to a thick doubler plate as part of a prequalified connection. Results were presented for a heat transfer analysis and an advanced modelling procedure was described for the stress analysis. Modelling parameters were based on the welding sequence currently used in practice based on information obtained from the industrial partner of this project.

This research project is in progress at the time of writing. The overall aim is to acquire information regarding the residual stresses, invoked by the welding process, leading to the formation of cracks in W-Shape column members. By means of a heat transfer analysis temperature values of all parts of the model can be obtained for each phase of the welding process while the results acquired by the stress analysis show promise and provide positive indication that the stress analysis model, once completed, will give a good indication of areas at risk of developing cracks. The stress analysis results available at present have given evidence that the welding process can cause significant deformations and thus stresses to the W-Shape section during fabrication. From this it can be assumed that a change in the welding sequence can greatly influence (reduce) the stresses developed. Considering that the welding sequence that was examined was the one currently used by welders in this type of connection, the importance of an accurate finite element model replicating these welding procedures is highlighted. Material testing will also be conducted on specimens obtained from the columns that experienced the crack formation; updated material properties will be inserted in the model. Moreover, within the framework of a parametric study, the influence of each welding parameter, e.g. preheat, interpass time, welding temperatures, number of weld passes, etc., will be investigated in order to make the developed modelling approach applicable to a wider range of welded connections. Finally, improvements to the current welding sequence will also be discussed.

Acknowledgements

The authors would like to thank ADF Group Inc. and DPHV Structural Consultants for their generous technical and financial support as well as the Natural Sciences and Engineering Research Council of Canada. Any opinions, findings, and conclusions or recommendations expressed in this paper are those of the authors and do not necessarily reflect the views of sponsors.

References

ABAQUS FEA/CAE (2011). 2010. Dassault Systemes Simulia Corp., Providence, RI, USA. @ Dassault Systèmes.

Aloraiera, A.S. and Joshib, S. and Asadic, M. and Alenac, R.G. and Goldakd, J.A. 2010. Microstructural and hardness modeling: Effect of multiple bead deposition in temper bead welding technique. *International Journal of Energy & Technology*, 2(16): 1-11.

Aloraier, A. and Ibrahim, R. and Thomson P. 2006. FCAW process to avoid the use of post weld heat treatment. *International Journal of Pressure Vessels and Piping*, 83: 394-398.

Blogdett, O.W. and Funderbur, R.S. and Miller, D.K. and Quintana M. 1999 *Fabricators and erectors guide to welded steel construction*, The James F. Lincoln Arc Welding Foundation, USA.

Brickstad, B. and Josefson, B.I. 1998. A parametric study of residual stresses in multi-pass buttwelded stainless steel pipes, *Journal of Pressure Vessel and Piping* 75: 11-25.

Chang, K. and Lee, C. 2009. Finite element analysis of the residual stresses in T-joint fillet welds made of similar and dissimilar steels. *The International Journal of Advanced Manufacturing Technology*, 41: 250-258.

Eurocode 3. 2005. Design of steel structures Part 1-2: General rules — Structural fire design.

Fisher, J.W. and Penser, A.W. 1987. Experience with Use of Heavy W Shapes in Tension. American Institut of Steel Construction.

Gunaraj, V. and Murugan, N. 2002. Prediction of Heat-Affected Zone Characteristics in Submerged Arc Welding of Structural Steel Pipes, *Welding Journal.*

Jin, J. and King, L.C. and Ping, C.S. and Shan, Z.M. 2011. Numerical modelling of the residual stress distributions in high strength steel plate-to-plate T and Y joint. *7th International Conference on Steel & Aluminium Structures*, Kuching, Sarawak, Malaysia.

Lee, C.S. and Chandel, R.S. and Seow, H.P. 2007. Effect of Welding Parameters on the Size of Heat Affected Zone of Submerged Arc Welding. *Materials and Manufacturing Processes*, Taylor & Francis, London, England.

Ma, N.X. and Ueda, Y. and Murakawa, H. and Madea, H. 1995. FEM analysis of 3D welding residual stresses and angular distortion in T-type fillet welds. *Transactions of the Japan Welding Research Institute,* 24(2):115–122.

Mark, A.F. and Francis, J.A. and Dai, H. and Turski, M. and Hurrell, P.R. and Bate, S.K. and Kornmeier, J.R. and Withers, P.J. 2012. On the evolution of local material properties and residual stress in a three-pass SA508 steel weld. *SciVerse Scinece Direct*, 60: 3268-3278.

Pilipenko, A. 2001. *Computer simulation of residual stress and distortion of thick plates in multi electrode submerged arc welding. Their mitigation techniques,* Department of Machine Design and Materials Technology Norwegian University of Science and Technology, N-7491 Trondheim, Norway.

Siddique, M. and Abid, M. and Junejo, H.F. and Mufti, R.A. 2005. 3-D finite element simulation of welding residual stresses in pipe-flange joints: effect of welding parameters. *Materials Science Forum*, 490–491:79–84

Suwan, S. 2002. *Analysis of structural plate mechanical properties: Statistical variability and implications in structural reliability,* Master of Science in Engineering Thesis, University of Texas, Austin.

Teng, T.L. and Fung, C.P. and Chang, P.H. and Yang, W.C. 2001. Analysis of residual stresses and distortions in T-joint fillet welds, *International Journal of Pressure Vessel and Piping,* 78:523-538.

Vakili-Tahami, F. and Zehsaz, M. and Saeimi-Sadigh, M and Seyedreyhani 2010. Finite Element Analysis of the In-service-Welding of T Joint Pipe Connections. *European Journal of Scientific Research,* ISSN, 1450-216X, 40(4): 557-568.

Vakili-Tahami, F. and Daei-Sorkhabi, A.H. and Saeimi-S, M.A. and Homayounfar, A. 3D finite element analysis of the residual stresses in butt-welded plates with modeling of the electrode-movement. *Journal of Zhejiang University Science A,* 10(1): 37-43.